

Remediation of low-density polyethylene (LDPE), and polyvinyl chloride (PVC) microplastics with porous sulfur polymers

Delia Teresa Sponza

Dokuz Eylül University, Engineering Faculty, Environmental Engineering Department, Buca İzmir Turkey

*Correspondence Author: Delia Teresa Sponza, Dokuz Eylül University, Engineering Faculty, Environmental Engineering Department, Buca İzmir Turkey.

Received Date: June 10, 2024 Accepted Date: June 20, 2024 Published Date: July 12, 2024.

Citation: Delia T. Sponza, (2024), Remediation of low-density polyethylene (LDPE), and polyvinyl chloride (PVC) microplastics with porous sulfur polymers, *Clinical Research and Clinical Reports*, 4(4); DOI:10.31579/2835-8325/084

Copyright: © 2024, Delia Teresa Sponza. This is an open-access article distributed under the terms of the Creative Commons Attribution License, which permits unrestricted use, distribution, and reproduction in any medium, provided the original author and source are credited.

Abstract

In this study, the phototransformation of low-density polyethylene (LDPE), and polyvinyl chloride (PVC) was promoted in porous sulfur polymer nanocomposite under sunlight. In order to investigate the potential photo catalytic effects of porous sulfur polymer the effects of some operational conditions on the photoremoval yields of during the transfer of LDPE and PVC were studied. 99% and 96% for LDPE and PVC yields was at a PB concentration of 3 mg/l, at LDPE and PVC concentrations of 400 mg/l a nanocomposite size and surface area of 10 micron and 0,098 m²/m, respectively, at 40 °C temperature a pH of 5.00 at a sun light power of 50 W/m². The FTIR analysis showed that the -SSH sulfanes groups porous sulfur polymers disappeared at 909 cm⁻¹ at So / PB mass ratios of 20:40 to 30: 60 and to 60:120. TGA analysis showed the thermal stability of the porous sulfur polymer nanocomposites. XRD analysis showed that the persistence of the nanocomposite with the presence of pure salt at 2θ=31°, 46°, 56°, and 66° after treatment.

Key words: low-density polyethylene (ldpe); polyvinyl chloride (pvc); porous sulfur polymer nanocomposite; photodegradation; microplastic

Introduction

Microplastics generated from the degradation of plastics in the environment due to sunlight, air, moisture, and heat [1,2]. They can contain some toxic compounds which can threaten the ecosystem. Flora and fauna can be exposed to the aforementioned pollutants and they can be ingested and eaten due to their minimized size like nanometer and micrometer.

[3,4]. This toxicity of some microplastics can cause inhibitions to the aquatic and terrestrial organisms. The presence of microplastics in wastewater was investigated by a lot of recent studies. The main source providing the disturbances and emissions of these pollutants was the surface runoff [5-7]. On the other hand, the concentrations of some personal care products containing fragments increased. Some microplastics cannot be treated in conventional treatment plants and some microplastics can be released to the rivers and to the oceans [8-10]. The existing technologies used in the wastewater treatment plants (coagulation, filtration, and advanced oxidation processes) cannot remove effectively and large volumes of wastewaters containing microplastics was discharged to the receiving water bodies. In last decades a lot of microplastic removal processes were developed for microplastic removal like adsorption, magnetic extraction, membrane filtration, coagulation and photodegradation [11-13]. Among these processes, photodegradation is a promising process to degrade the microplastics under UV light. Under this light, the electrons in the nanocomposites are activated and generate electron-hole pairs resulting in reactive oxidizing species (ROS). These species can then break down the microplastics into harmless byproducts, such as carbon dioxide and water.

Polymeric materials such as low-density polyethylene (LDPE), high-density polyethylene (HDPE), polypropylene (PP), polyethylene terephthalate

(PET), polystyrene (PS), and polyvinyl chloride (PVC) are common materials under study due to their widespread use, particularly in the packaging industry, which contributes to microplastic pollution in the world [14-17]. The biodegradability of microplastic-based materials like polyurethanes (PU), polylactic acid (PLA), nylon, polycarbonates, and were studied [18-20]. Microplastics are decomposed through photodegradation and possible biodegradation, [21-24]. The physicochemical properties of polymers depend on environmental conditions such as weather conditions, temperature, irradiation and pH values. Microplastics in aqueous bodies are a potential threat to aquatic species and they were considered an emerging contaminant. They are not degraded, and they can adhere to animals when they enter the food chain. On the other hand, they can adsorb some harmful pollutants.

Sulfur polymers have numerous applications like optoelectronic, superhydrophobic materials, and photochemical materials, biopolymers and proton-conducting electrolytes. The porous sulfur-containing polymers can be used to adsorb the heavy metals. On the other hand, the photoactive properties of sulfur-containing polymers were reported. The porous sulfur-containing polymers were used for removing organic contaminants from pharmaceuticals, personal care products, and endocrine disruptors.

In this study low-density polyethylene (LDPE), and polyvinyl chloride (PVC) microplastics were chosen to remediate them with porous sulfur-containing polymer using 1,3-diisopropenylbenzene via photodegradation. The effects of some operational parameters like concentration of pollutants and nanocomposite, surface area of nanocomposite, temperature, pH and light intensity on the photodegradation yields of LDPE and PVC were studied.

Material and Methods

Production of porous sulfur-containing polymer nanocomposite

Elemental sulfur was heated under 190–210 °C in a magnetic stirring. Once completely molten then certain amount of 1,3-diisopropenylbenzene (PB) was added. S^o / PB mass ratio was varied from 20:40 to 30: 60 and to 60:120. The component was stirred, the still-liquid pre-polymer was transferred in a silicone cap. The mixture was blended and it was maintained at 160 °C for 6 h.

Characterization of porous sulfur-containing polymer nanocomposite

To characterization of porous sulfur-containing polymer, nitrogen adsorption/desorption isotherms were acquired at 79 K using a surface area analyzer (NOVA). Scanning Electron Microscopy (SEM) imaging and Energy-Dispersive X-ray Spectroscopy (EDS) were performed using an FEI Inspect F system with an operational acceleration voltage of 10–20 kV. Fourier transformed infrared (FTIR) spectra were recorded using a Bruker Tensor 27 instrument over the wavenumber range of 500 to 4000 cm⁻¹. Powder X-ray diffraction patterns were performed by Panalytical X'Pert PRO MPD equipped PIXcel detector. Cu K α radiation was utilized, and data were collected over a range of 5–70° using loose powder samples on thin Mylar film within aluminium well plates. Thermogravimetric analysis (TGA) (was conducted under an inert atmosphere on a TA Instruments TGA 5500. Heating was carried out at a heating rate of 10 °C min⁻¹, from room temperature to 600 °C.

Analytical Measurements

LDPE and PVC were analyzed by a gas chromatograph with a flame ionization detector using a TRACE GC gas chromatograph. It was provided with a 30 m \times 0.32 mm Rtx-1 column.

Photocatalytic studies

Photocatalytic experiments were carried out in a laboratory scale reactor made of quartz with a volume of 3 l. The photoreactor was a vertical tubular reactor, and the treated solution was circulated by a peristaltic pump operating with a speed of 20 l h⁻¹. The loop contained also a sampling port and was fed with air at a rate of (2,0 cm³ s⁻¹).

Results and Discussion

FTIR analysis results

Te extent of PB mass ration (60 and 120) indicates the consumption of double bonds during the crosslinking process (Figure 1). The -SSH sulfanes groups also in porous sulfur polymers disappeared at 909 cm⁻¹ band in the FTIR spectra at S^o / PB mass ratios of 20:40 to 30: 60 and to 60:120 (Figure 1). As a result, of polymerization the peaks associated with sulphur monomer exhibited maximal peaks at 698 cm⁻¹ band in the FTIR spectra (Figure 1). This showed the presence that C-S bond formation. The exhibited the peaks relevant to sulfur comonomer units which has an appearance at 690 cm⁻¹ band in the FTIR spectra, illustrating the C-S bonds

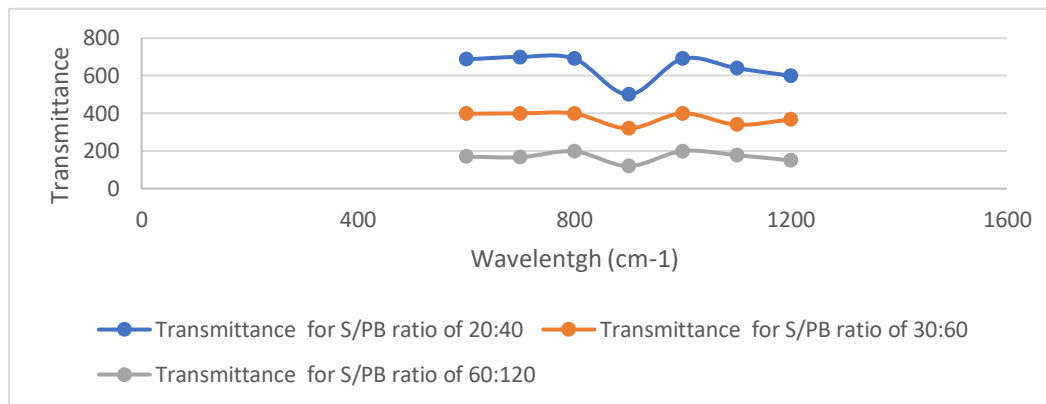


Figure 1: FTIR analysis results of PB nanocomposite at different S/ PB ratios

TGA analysis results

In order to detect the thermal stability of porous sulfur polymers (PB), TGA analysis were performed. Figure 2 illustrates TGA thermograms of porous sulfur polymers at different percentages of varying weight percentages of sulfur and PB. The graph depicts that the degradation of pure sulfur

commences at approximately 190 °C, with complete weight loss (100%) observed around 283 °C. However, the PB exhibited a higher decomposition temperature than pure sulfur. Additionally, the PB had a residue at 600 °C, and this residual content increased with a rise in pollutant content within the composition.

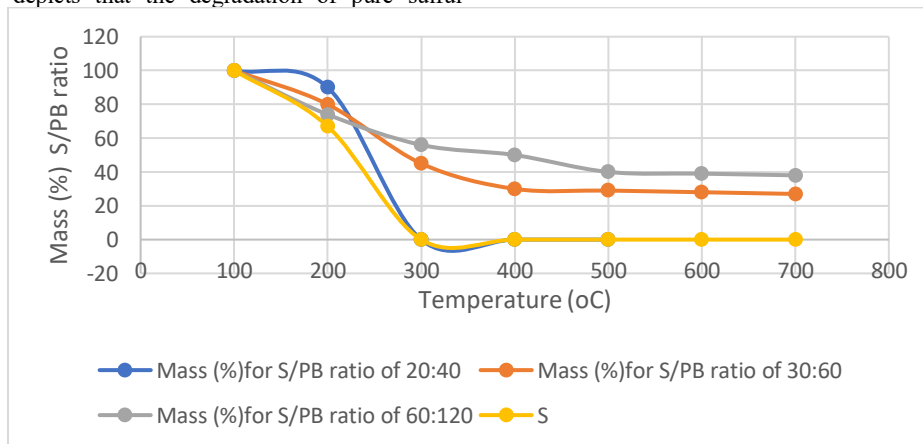


Figure 2: TGA analysis results

XRD analysis results

XRD patterns for pure sulfur and porous sulfur polymer nanocomposite after water treatment are presented in Figure 3. In the case of pure sulfur,

characteristic diffraction peaks were discernible at $2\theta=23^\circ$, 27° , 28° , 53° , and 56° . However, these peaks were absent following the copolymerization reaction in polymers containing over 60% PB content. This absence suggests

a transformation from crystalline monoclinic sulfur to a highly cross-linked amorphous copolymer structure. The diffraction peaks originating from pure salt (at $2\theta=31^\circ$, 46° , 56° , and 66°) remained observable in PB after water treatment. This persistence indicates the presence of residual table salt even after the water washing treatment.

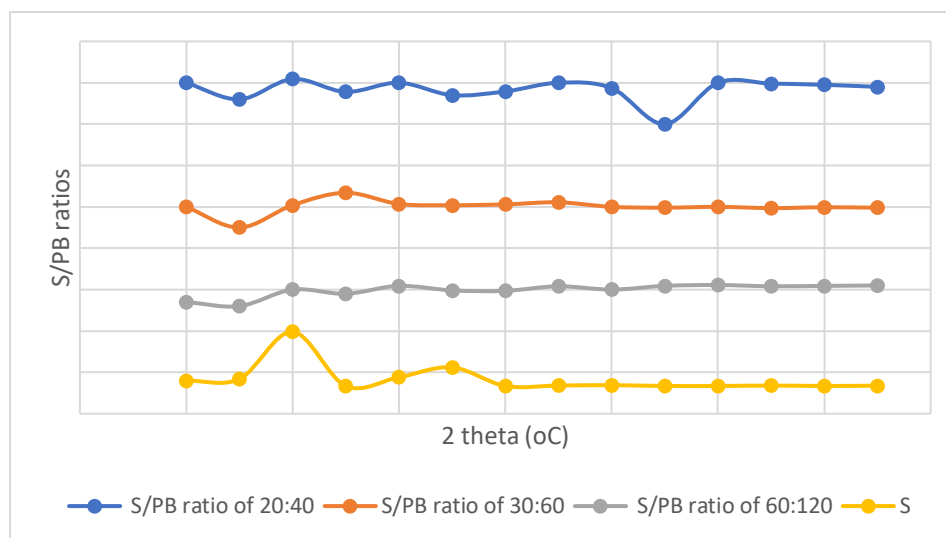


Figure 3: XRD analysis results

SEM analysis results

SEM images of raw PB with a S^o to PB mass ratio of 20:40 before treatment indicated the presence of a non-porous surface (Figure 4a). The SEM image indicates homogenous disturbances of salt and sulfur in the PS

nanocomposite. After treatment, these salts were dissolved and a porous structure was generated (Figure 4b). The non homogenous structure of pore can be increased with salt. Figure 4c showed that the pores sizes increased. This increases the surface contour of the porous media for increase the adsorption process at the beginning of photodegradation. [29-30].

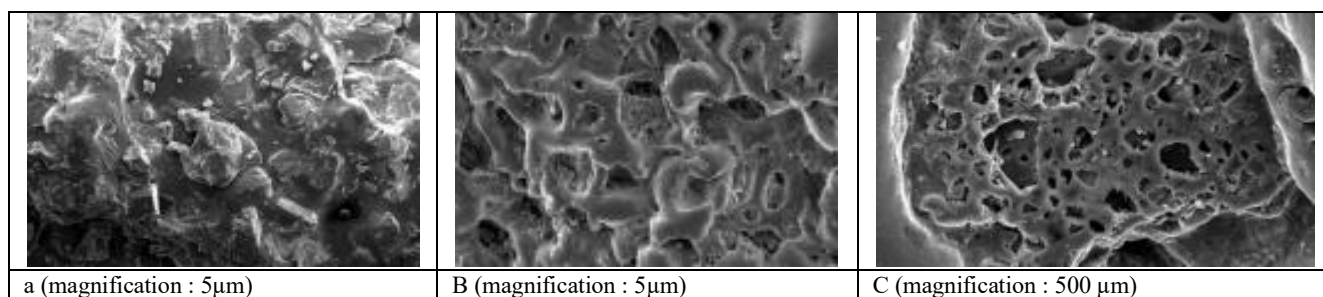


Figure 4: SEM image of porous sulfur polymers at a S^o / PB mass ratio of 20:40 in raw PB (a), treated PB (b), treated PB(c)

Effects of nanocomposite concentration

The PB nanocomposite concentration was increased from 1 mg/l up to 5 mg/l with a S/PB ratio of 20:40 to detect the optimal nanocomposite dose for maximal LDPE and PVC photodegradation yields. The photocatalytic activity of LDPE and PVC enhanced when the PB concentration was increased from 1 mg/l to 2 and 3 mg/l (Table 1). The yields reached from 70% - 72% to 84% and 88% and to 99% and 96% for LDPE and PVC at a PB concentration of 3 mg/l. Further increase of PB nanocomposite concentration showed slightly lowest photocatalytic activity. The LDPE

and PVC yields decreased to 84% and 81% at 5 mg/l PB nanocomposite concentration. The photodegradation yields of LDPE and PVC pollutants are influenced by the active site and the photoabsorption of the catalyst used. Adequate loading of PB nanocomposite increases the generation rate of electron/hole pairs for enhancing the photodegradation of LDPE and PVC microplastics. High dose of the PB lowered the light penetration and reduces the photodegradation percentages of pollutants. At high PB nanocomposite concentration the surface area decreased while the size of the nanocomposite increased [31-33].

PB nanocomposite concentration (mg/l)	LDPE Photodegradation yields (%)	PVC Photodegradation yields(%)
1	72	70
2	88	84
3	99	96
4	94	90
5	84	81

Table 1: Effect of nanocomposite concentration on the photodegradation yields

Effect of LDPE and PVC concentrations

The effect of initial pollutant concentration on the photocatalytic degradation is illustrated in Table 2. It was observed that the photodegradation efficiency

as a function increasing pollutant concentration. At 50, 100, 200 and 400 mg/l LDPE and PVC concentrations the yields recorded between 98-99% and 95-96%, respectively for LDPE and PVC. When the pollutant concentrations were increased to 500 and 700 mg/l irradiation was not

adequate to complete the degradation of the pollutants. The yields of pollutants decreased to 85-89% and to 79-75% for LDPE and PVC [34,35].

LPDE and PVC concentrations (mg/l)	LDPE Photodegradation yields(%)	PVC Photodegradation yields(%)
50	99	97
100	98	98
200	99	97
400	99	98
500	89	79
700	85	75

Table 2: Effect of pollutant concentration on the photodegradation yields

Effect of surface area

The PB nanocomposite surface area significantly affects the pollutant removal efficiencies during the photodegradation during photocatalysis. The activity of PB depends on the holes and electron during activation of PB nanocomposite. Small particle sized PB nanocomposite (10 nm) sizes translate to reduced distance transferring the electrons and holes during

photocatalysis ending with high LDPE and PVC photodegradation yields (99% and 96%) (Table 3). PB Nanocomposites with a size 40 nm the PB exhibited high photodegradation yields (98% and 95%).

In this study negligible weight losses were observed for PB nanocomposite resulting in, surface area effect of photodegradation yields was not significant.

PB anocomposite size (micron) and surface area (m ² /m)	LDPE Photodegradation yields(%)	PVC Photodegradation yields (%)
10, 0,098	99	96
40, 0,178	90	82
100, 0,234	88	79

Table 3: Effect of nanocomposite size and surface on the photodegradation yield

Effect of temperature

The temperature was increased from 20 oC up to 25, 30 and 40 Oc. At 20 oc the PLDE and PVC yields was accounted as 94% and 97%, respectively. As the temperature was increased to 40 Oc the LDPE and PVC yields reached

to a maximum (99% and 97%) (Table 4). Generally, at high temperatures like 80°C, there is ecombination of charge carriers, ending with inhibition of photodegradation. As the temperature was increased to 40°C the photocatalytic activity increased since the kinetic energy for the reactive species elevated [36].

Temperature (Oc)	LDPE Photodegradation yields (%)	PVC Photodegradation yields (%)
20	72	70
25	88	83
30	90	86
40	99	97
80	60	52

Table 4: Effect of temperature on the photodegradation yields

Effect of pH

The formation of reactive oxidizing species by photocatalyst depends to pH. The pH influences the electrical double-layer charge at the solid electrolyte interface, affecting the formation of the electron-hole pairs on the surface of

the photocatalyst [32-34]. Variation in pH modifies the potentials of catalytic processes. The surface of PB nanocomposite is positively charged at pH= 5 and negatively charged in apH of 8 (Table 5). LDPE and PVC exhibited crystalline structure and exhibited high photodegradation yields at pH=5.

PB nanocomposite concentration (mg/l)	LDPE Photodegradation yields(%)	PVC Photodegradation yields(%)
4	89	85
5	99	96
6	93	90
7	67	60
8	45	40

Table 5: Effect of pH on the photodegradation yields

Effect of sun lighth

The wavelength and intensity of sunlighth affect significantly the the photodegradation of LDPE and PVC. The sun light is stronger than visible light because its waves are shorter than those of visible light. Therefore, it has higher efficiency in the photo degradation of microplastics. The number of photons available for activating the catalyst surface was relevant with sun intensity. The lower the intensity, the lower the activation energy; as a result,

low photodegradation efficiency is observed. With an increase in intensity, more active sites are activated increasing the interactions between the catalyst and the adsorbed substrate on its surface, hence higher degradation rates are attained. In this study it was found that the photodegradation yields of LDPE and PVC were maximum at a sun lighth intensity of 50 W/ m² compared to 20 W/m² (Table 6)

Sun Ligth (W/m ²)	LDPE Photodegradation yields(%)	PVC Photodegradation yields(%)
20	62	58

30	84	80
40	90	85
50	99	96

Table 6: Effect of sun power on the photodegradation yields**Conclusions**

In this study two microplastics namely low-density polyethylene (LDPE), and polyvinyl chloride (PVC) was photodegraded by porous sulfur polymer nanocomposite under optimized conditions. High photodegradation yields as high as 99% and 97% was detected for LPDE and PVC, respectively. This nano composited can be suggested to the photo removal of other microplastics degraded with difficulty at short times.

References

- Gogoi A, Mazumder P, Tyagi VK, Chaminda GT, An AK, Kumar M. (2018). Occurrence and fate of emerging contaminants in water environment: A review. *Groundw Sustain Dev*, 6:169-180.
- Liu X, Shi H, Xie B, Dionysiou DD, Zhao Y. (2019). Microplastics as both a sink and a source of bisphenol A in the marine environment. *Environ Sci Technol*, 53:10188-10196.
- Wu P, Tang Y, Jin H, Song Y, Liu Y, Cai Z. (2020). Consequential fate of bisphenol-attached PVC microplastics in water and simulated intestinal fluids. *Environ Sci Ecotechnology*, 2: 100027.
- Song X, Zhuang W, Cui H, Liu M, Gao T, Li A, et al. (2022). Interactions of microplastics with organic, inorganic and bio-pollutants and the ecotoxicological effects on terrestrial and aquatic organisms. *Sci Total Environ*, 838:156068.
- Campanale C, Massarelli C, Savino I, Locaputo V, Uricchio VF. (2020). A detailed review study on potential effects of microplastics and additives of concern on human health. *Int J Environ Res Public Health*, 17: 1212.
- Yaseen A, Assad I, Sofi MS, Hashmi MZ, Bhat SU. (2022). A global review of microplastics in wastewater treatment plants: Understanding their occurrence, fate and impact. *Environ Res*, 212:113258.
- Gatidou G, Arvaniti OS, Stasinakis AS. (2019). Review on the occurrence and fate of microplastics in sewage treatment plants. *J Hazard Mater*, 367:504-512.
- Habib RZ, Thiemann T, Al Kendi R. (2020). Microplastics and wastewater treatment plants—A review. *J Water Resour Prot*, 12:97637.
- Wang C, O'Connor D, Wang L, Wu WM, Luo J, Hou D. (2022). Microplastics in urban runoff: Global occurrence and fate. *Water Res*, 225: 119129.
- Han N, Zhao Q, Ao H, Hu H, Wu C. (2022). Horizontal transport of macro- and microplastics on soil surface by rainfall induced surface runoff as affected by vegetations. *Sci Total Environ*, 831:154989.
- Lu Y, Li MC, Lee J, Liu C, Mei C. (2023). Microplastic remediation technologies in water and wastewater treatment processes: Current status and future perspectives. *Sci Total Environ*, 868: 161618.
- Liu W, Zhang J, Liu H, Guo X, Zhang X, Yao X, et al. (2021). A review of the removal of microplastics in global wastewater treatment plants: Characteristics and mechanisms. *Environ Int*, 146: 106277.
- Kwon HJ, Hidayatullah H, Peera SG, Lee TG. (2022). Elimination of microplastics at different stages in wastewater treatment plants. *Water*, 14: 2404.
- Wang J, Sun C, Huang QX, Chi Y, Yan JH. (2021). Adsorption and thermal degradation of microplastics from aqueous solutions by Mg/Zn modified magnetic biochars. *J Hazard Mater*, 419.
- Liu F, Nord NB, Bester K, Vollertsen J. (2020). Microplastics removal from treated wastewater by a biofilter. *Water*, 12:1085.
- Wang L, Kaeppler A, Fischer D, Simmchen J. (2019). Photocatalytic TiO₂ micromotors for removal of microplastics and suspended matter. *ACS Appl Mater Interfaces*, 11: 32937-32944.
- Uheida A, Mejia HG, Abdel-Rehim M, Hamd W, Dutta J. (2021). Visible light photocatalytic degradation of polypropylene microplastics in a continuous water flow system. *J Hazard Mater*, 406:124299.
- Xu Q, Huang QS, Luo TY, Wu RL, Wei W, Ni BJ. (2021). Coagulation removal and photocatalytic degradation of microplastics in urban waters. *Chem Eng J*, 416: 129123.
- Ebrahimbabaei P, Yousefi K, Pichtel J. (2022). Photocatalytic and biological technologies for elimination of microplastics in water: Current status. *Sci Total Environ*, 806: 150603.
- Ouyang Z, Yang Y, Zhang C, Zhu S, Qin L, Wang W, et al. (2021). Recent advances in photocatalytic degradation of plastics and plastic-derived chemicals. *J Mater Chem A*, 9: 13402-13441.
- Ge J, Zhang Z, Ouyang Z, Shang M, Liu P, Li H, et al. (2022). Photocatalytic degradation of (micro) plastics using TiO₂-based and other catalysts: Properties, influencing factor, and mechanism. *Environ Res*, 209: 112729.
- Devi MK, Karmegam N, Manikandan S, Subbaiya R, Song H, Kwon EE, et al. (2022). Removal of nanoplastics in water treatment processes: A review. *Sci Total Environ*, 845: 157168.
- Mukherjee PS, Ray AK. (1999). Major challenges in the design of a large-scale photocatalytic reactor for water treatment. *Chem Eng Technol*, 22: 253-260.
- Shen M, Song B, Zhou C, Hu T, Zeng G, Zhang Y. (2022). Advanced oxidation processes for the elimination of microplastics from aqueous systems: Assessment of efficiency, perspectives and limitations. *Sci Total Environ*, 842: 156723.
- Rodriguez-Narvaez OM, Goonetilleke A, Perez L, Bandala ER. (2021). Engineered technologies for the separation and degradation of microplastics in water: A review. *Chem Eng J*, 414: 128692.
- Xie A, Jin M, Zhu J, Zhou Q, Fu L, Wu W. (2023). Photocatalytic technologies for transformation and degradation of microplastics in the environment: Current achievements and future prospects. *Catalysts*, 13: 846.
- Du H, Xie Y, Wang J. (2021). Microplastic degradation methods and corresponding degradation mechanism: Research status and future perspectives. *J Hazard Mater*, 418: 12637.
- Gewert B, Plassmann MM, MacLeod M. (2015). Pathways for degradation of plastic polymers floating in the marine environment. *Environ Sci*, 17: 1513-1521.
- Tofa TS, Kunjali KL, Paul S, Dutta J. (2019). Visible light photocatalytic degradation of microplastic residues with zinc oxide nanorods. *Environ Chem Lett*, 17:1341-1346.
- Ariza-Tarazona MC, Villarreal-Chiu JF, Barbieri V, Siligardi C, Cedillo-González EI. (2019). New strategy for microplastic degradation: Green photocatalysis using a protein-based porous N-TiO₂ semiconductor. *Ceram Int*, 45: 9618-9624.
- Ariza-Tarazona MC, Villarreal-Chiu JF, Hernández-López JM, De la Rosa JR, Barbieri V, Siligardi C, et al. (2020). Microplastic pollution reduction by a carbon and nitrogen-doped TiO₂: Effect of pH and temperature in the photocatalytic degradation process. *J Hazard Mater*, 395: 122632.
- Allé PH, Garcia-Muñoz P, Adouby K, Keller N, Robert D. (2021). Efficient photocatalytic mineralization of

- polymethylmethacrylate and polystyrene nanoplastics by TiO₂/β-SiC alveolar foams. *Environ Chem Lett*, 19: 1803-1808.
33. Yuwendi Y, Ibadurrohman M, Setiadi S, Slamet S. (2022). Photocatalytic degradation of polyethylene microplastics and disinfection of *E. coli* in water over Fe-and Ag-modified TiO₂ nanotubes. *Bull Chem React Eng Catal*, 17: 263-277.
34. Ali SS, Qazi IA, Arshad M, Khan Z, Voice TC, Mehmood CT. (2016). Photocatalytic degradation of low-density polyethylene (LDPE) films using titania nanotubes. *Environ Nanotechnol Monit Manag*, 5: 44-53.
35. Llorente-García BE, Hernández-López JM, Zaldívar-Cadena AA, Siligardi C, Cedillo-González EI. (2020). First insights into photocatalytic degradation of HDPE and LDPE microplastics by a mesoporous N-TiO₂ coating: Effect of size and shape of microplastics. *Coatings*, 10: 658.
36. Tofa TS, Kunjali KL, Paul S, Dutta J. (2019). Visible light photocatalytic degradation of microplastic residues with zinc oxide nanorods. *Environ Chem Lett*, 17: 1341-1346.

Ready to submit your research? Choose ClinicSearch and benefit from:

- fast, convenient online submission
- rigorous peer review by experienced research in your field
- rapid publication on acceptance
- authors retain copyrights
- unique DOI for all articles
- immediate, unrestricted online access

At ClinicSearch, research is always in progress.

Learn more <https://clinicsearchonline.org/journals/clinical-research-and-clinical-reports>



© The Author(s) 2024. **Open Access** This article is licensed under a Creative Commons Attribution 4.0 International License, which permits use, sharing, adaptation, distribution and reproduction in any medium or format, as long as you give appropriate credit to the original author(s) and the source, provide a link to the Creative Commons licence, and indicate if changes were made. The images or other third party material in this article are included in the article's Creative Commons licence, unless indicated otherwise in a credit line to the material. If material is not included in the article's Creative Commons licence and your intended use is not permitted by statutory regulation or exceeds the permitted use, you will need to obtain permission directly from the copyright holder. To view a copy of this licence, visit <http://creativecommons.org/licenses/by/4.0/>. The Creative Commons Public Domain Dedication waiver (<http://creativecommons.org/publicdomain/zero/1.0/>) applies to the data made available in this article, unless otherwise stated in a credit line to the data.